

Multilayer Polymer Particles with Periodic Modulation in Refractive Index

Armin Alteheld, Ilya Gourevich, Lora M. Field, Chantal Paquet, and Eugenia Kumacheva*

Department of Chemistry, University of Toronto, 80 Saint George Street, Toronto, Ontario, M5S 3H6 Canada

Received December 12, 2004; Revised Manuscript Received January 21, 2005

ABSTRACT: We report synthesis of polymer particles comprising layers with alternating high and low refractive index. We used poly(heptafluorobutyl methacrylate) as the low refractive index component and polystyrene as the high refractive index counterpart. We employed a copolymerization approach, the addition of a phase transfer catalyst (cyclodextrin), and a mixed initiator approach to produce spherical particles with a well-defined morphology. The composition and morphology of these particles were proven by DSC, XPS, NMR, and SEM. The refractive index contrast between these alternating high and low refractive index layers was ca. 0.20 ± 0.018 . This work shows a route toward synthesis of polymeric spherical dielectric resonators.

Introduction

Recently, macroscopic materials with periodically modulated composition and structure have attracted immense interest due their unique interactions with light. These materials show promising applications as optical limiting, three-dimensional optical data storage, security data encryption, and chemical and biochemical sensing.^{1–23} In particular, photonic band gap materials rely on a strong periodic modulation in refractive index, which under Bragg's conditions, prohibits propagation of light in a particular direction.⁴ The required periodicity of macroscopic materials is often achieved using self-assembly of inorganic or polymer colloid particles into periodic one-, two-, or three-dimensional arrays.⁵ This strategy, however, has a deficiency in control of periodicity of the material over large length scales.

The concept of another class of materials relies on *isolated* dielectric particles with radially periodic variation in refractive indices.⁶ In such particles the reflectivity at a single interface between two layers is only $|2\Delta n/n|^2$, where Δn is the refractive index difference and n the average refractive index. Yet, inhibited light propagation can be achieved in such systems even if there is only a weak modulation in the refractive index. When N interfaces are spaced so that reflection from each interface adds in phase at a given wavelength, the reflectivity grows with N as $|2N\Delta n/n|^2$ until it approaches unity and light is completely rejected from the material. Thus, even for a small value of Δn , a sufficiently large N can lead to novel optical properties of the particles.

Since the prediction of multilayer dielectric resonators was made, the experimental proof of the novel optical properties of the dielectric graded spheres has remained a synthetic challenge. Several attempts have been made to obtain inorganic microspheres (e.g., particles composed of SiO_2 and $\text{Si}^{7,8}$). No effort, however, has been made to synthesize multilayer polymer spheres with a periodic modulation in refractive index.

Despite a significant progress in the design, synthesis, and fabrication of core-shell and multilayer polymeric particles, most of these works purposely avoided the

synthesis of particles with a strong contrast in refractive indices of the constituent polymers.^{1b,2,9,10} We note that strong light scattering is expected from such particles and the resulting macroscopic materials, e.g., polymeric films.

Regardless of the difference in optical properties of the core- and shell-forming polymers, the challenge in synthesis of the multilayer particles was achieving good compatibility between the layers. Depending on the value of interfacial tension between the phases, the constituent polymers could be completely phase separated (that is, they formed several types of particles) or their formed multiphase particles with peculiar non-spherical morphologies.¹¹ The compatibility between the constituent polymers has been enhanced by modifying the compositions of the polymers,¹² by using compatibilizers,¹³ or by employing grafted macromonomers in the synthesis of the polymer shells.¹⁴ In addition, the morphology of the particles could be controlled by varying the reaction temperature, cross-linking density, monomer feeding rate, and glass transition temperatures of core- and shell-forming polymers.¹⁵

In the current work, we report synthesis of polymer multilayer microspheres with strong periodic modulation in refractive index of the layers. We note that the design and synthesis of graded polymer resonators is a complex task: the required thickness and number of layers change with refractive index, that is, polymer composition and the wavelengths to be used. Here we present the first attempt to use poly(heptafluorobutyl methacrylate) (PHFBMA, $n \approx 1.38$, $\lambda = 590 \text{ nm}$)¹⁶ as a low refractive index component and polystyrene (PS, $n \approx 1.59$, $\lambda = 589 \text{ nm}$)¹⁷ as a high refractive index counterpart yielding polymer particle with periodically modulated refractive index. We employed multistage emulsion polymerization with several important features. First, we used a mixture of methyl- β -cyclodextrin (phase transfer catalysts)¹⁸ and water as a reaction medium. Second, we employed a copolymerization approach:¹⁹ each layer contained a small fraction of the counterpart polymer. Using this method, we achieved a more gradual change in interfacial tension between the layers (though slightly compromising in the value

Table 1. Synthesis of Multilayer Particles Using Multistage Emulsion Polymerization

sample ^a	precharge			pumping mixture				ionic initiator solution			
	water (g)	seed(g)	β -cyclo-dextrin (mg)	styrene (g)	HFBMA (g)	EGDMA (uL)	AIBN (mg)	KPS (mg)	water (g)	coagulate (g)	temp (°C)
1a	744.4		281	5.06	0.56	19.1		750			70
1b	372.2			2.82		10.2		375			70
1c	49.25		37.5	0.75				100			70
1d	49.25		37.5	0.075	0.675			100			70
1e	49.25		37.5	0.675	0.075			100			70
1f	49.25		37.5		0.75			100			70
2a	50	1a	50	500	0.50	4.50	8.1	100	79	1.0	80
2b	50	1b	50	500		5.00	8.1	100 ^c		2.9	80
3a	60	2a ^b	40	200	3.60	0.40	13.5	80	3	65	80
4a	40	3a ^b	40	200	0.20	1.80	3.30	40		20	80
5a	40	4a ^b	40	50	0.90	0.10	3.4	20	0.75	40	80

^a The first left column shows the labels of samples synthesized in different stages. The first number in sample labels gives the reaction stage (1 to 5). The letter adjacent to this number corresponds to various recipes used for the same stage. ^b Seeds were purified by centrifugation (3 \times) prior to polymerization. The solid content of the dispersion of purified seeds was (2a) 1.76 ± 0.02 wt %, (3a) 1.15 ± 0.01 wt %, and (4a) 1.09 ± 0.00 wt %. ^c Because of low solubility of AIBN in water, 50 mg was dispersed in the precharge mixture and 50 mg was dissolved in a monomer mixture.

of Δn). Finally, we used a mixed initiator approach.²⁰ Using a combination of these methods, we synthesized four-layer microspheres with periodically varying composition and properties. We note that the resulting polymer microspheres can be used either in their own right as the *isolated* dielectric resonators, or they can be employed for the production of polymeric macroscopic materials with periodic modulation in refractive index. So far, the latter materials have been obtained by infiltrating a high refractive index polymer or monomer in the interstitial voids.²¹

Experimental Section

Materials. Methyl- β -cyclodextrin (average $M_n = 1310$, 1.6–2.0 CH₂ groups per unit anhydroglucose) and ethylene glycol dimethacrylate (EGDMA, 98%) were purchased from Aldrich Canada and used without further purification. Styrene (99%, Aldrich Canada) was distilled before use. Potassium persulfate (KPS, >98%, BDH Chemicals Ltd.) and 2,2'-azobis(2-methylpropionitrile) (AIBN, VAZO 64, DuPont Canada) were used as received. Deionized water was purified by using a Millipore Milli-Q Plus purification system (Millipore Corp.). 2,2,3,3,4,4,4-Heptafluorobutyl methacrylate (HFBMA) was synthesized as described elsewhere.²² Tetrahydrofuran-*d*₈ (99.5 atom % D) was purchased from Isotech Inc. and used as received.

Latex Preparation. The multilayer latex particles were prepared using a multistage surfactant-free emulsion polymerization technique. All reactions were carried under nitrogen pressure in a double-walled three-neck flask equipped with a reflux condenser, a nitrogen inlet, and a mechanical stirrer. The reaction temperature was controlled using temperature-controlled water baths. Particle polymerization in the first stage (synthesis of latex cores) was performed at 70 ± 0.1 °C; further polymerization stages were conducted at 80 ± 0.1 °C.

Batch Synthesis of Homopolymer Seeds. The reactor was charged with water, the cross-linking agent EGDMA, and the degassed monomer (styrene or HFBMA) and purged with nitrogen for 30 min. An aqueous solution of KPS was injected in the reactor with a syringe. The temperature of the mixture was increased to 70 ± 0.1 °C. The reaction was carried out for 3 h.

Semicontinuous Synthesis of Copolymer Seeds. The reactor was charged with water, KPS, and methyl- β -cyclodextrin and purged with nitrogen for 30 min. The degassed mixture of styrene, HFBMA, and EGDMA was introduced into the reactor using a fluid-metering pump at a rate of 0.11 mL/min. After feeding was complete, the reaction was carried out for 3 h.

Synthesis of Multilayer Particles. Latex dispersion from the previous stage, water, and methyl- β -cyclodextrin were mixed in the reaction flask. The monomer mixture, EGDMA, and AIBN were introduced into the reactor using a fluid-metering

pump at a rate of 0.09 mL/min. An aqueous solution of KPS was added simultaneously with the monomer mixture using the second fluid-metering pump. The reaction was carried out for 3 h after the feeding stage was complete. After cooling to room temperature, the suspensions were filtered to remove agglomerate.

The recipes for the synthesis of the seeds and the multilayer particles are given in Table 1. A five-stage polymerization series resulted in the preparation of particles with a core and four layers of alternating compositions.

In Table 1 polymer latex cores were synthesized from polystyrene (1b), PHFBMA (1f), or a copolymer of styrene and HFBMA (1a). Non-cross-linked particles (1c, 1d, 1e) with varying comonomer ratios were used to determine the value of refractive index of polymers with different compositions.

In stage 2 the low refractive index layer composed of a copolymer PHFBMA-PS or PHFBMA was polymerized on the surface of the cores (samples 2a and 2b, respectively). In the third and the fifth stages a high refractive index layer (enriched with PS) was synthesized on the surface of the preceding low refractive index layer enriched with PHFBMA; in stage 4 a layer enriched with PHFBMA was synthesized.

Characterization of Particle Composition. *Analysis of Bulk Composition of Multilayer Particles.* The bulk composition of microspheres was analyzed by proton magnetic resonance spectroscopy (¹H NMR) using a Varian Unity 500 spectrometer. The aqueous suspensions were centrifuged and redispersed five times. The microspheres were dried at room temperature and redispersed in tetrahydrofuran-*d*₈. The molar ratio of monomeric units was calculated using the normalized integral of aromatic hydrogens related to styrene (δ /ppm: 6.2–7.6) and the methylene units of (PHFBMA) side groups (δ /ppm: 4.3–4.9).

Analysis of Surface Composition of Multilayer Particles. Analysis of the particle surface composition was performed by X-ray photoelectron spectroscopy (XPS) using a Leybold "MAX200" apparatus. Prior to experiments, the aqueous suspensions were centrifuged and redispersed five times. The particles were deposited on glass slides by evaporating the suspension at room temperature. The samples were excited with a dual-anode Mg radiation source using an aperture of 4×7 mm², and the relative amount of fluorine-to-carbon was determined. The copolymer composition was calculated by correlating the experimental atomic fluorine content to the molar ratio of fluorine-to-carbon in HFBMA and the number of atoms in both repeating units.²³

Thermal Analysis of Multilayer Particles. A differential scanning calorimeter (model DSC Q100, TA Instruments-Waters) was used for measurements of the glass transition temperatures (T_g) of polymers. The samples were equilibrated at 30.0 °C, heated to 150.0 °C at a rate 10.0 °C/min, and then

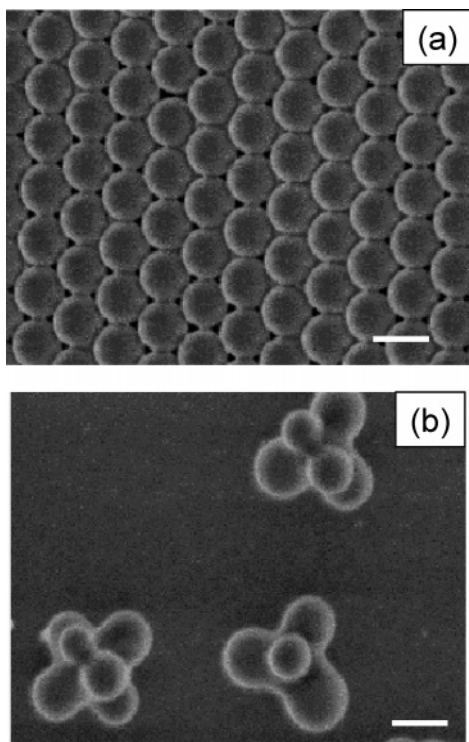


Figure 1. Typical SEM images of PS cores (a) and PS-PHFBMA particles (b) (samples 1b and 2b, respectively). Scale bar is 200 nm.

cooled at a ramp of 10.0 °C/min to 30.0 °C. Then the samples were reheated to 160 °C at 10.0 °C/min for the measurements of T_g .

Determination of Polymer Refractive Indices. Dispersions of non-cross-linked microspheres were centrifuged and redispersed five times. The microspheres were dried at room temperature, dissolved in ethyl acetate or chlorobenzene to concentration of ca. 5 wt %, and spin-coated on single-side polished silicon wafers. A Sopra GES-5 spectroscopic ellipsometer was used to acquire γ and Δ from 0.62 to 4.9 eV at angles of incidence of 65°, 70°, and 75°. The Levenberg-Marquardt regression algorithm was used to find the minimum difference between the acquired Y and D curves and the data generated from an optical model. The model consisted of three layers: a homogeneous crystalline Si substrate, a 2 nm SiO₂ layer, and the polymer layer. The refractive index and the absorptivity of the polymer layer were modeled using a Cauchy dispersion law.

Particle Size and Shape Characterization. The shapes of latex particles were examined by scanning electron microscopy (SEM, Hitachi S-5200 scanning electron microscope) at an accelerating voltage of 1.0 kV and a current of 10 mA. A droplet of a dilute latex dispersion was dried on a carbon-coated copper TEM grid.

Dimensions of homogeneous latex particles were determined by photon correlation spectroscopy using a Zetasizer 3000 apparatus (Malvern Instruments, Malvern, UK) or SEM. In the first case, the instrument used a 10 mW helium-neon laser at a wavelength of 632.8 nm. Scattered light was collected at an angle of 90° by a photon counting photomultiplier tube. The samples were purified by centrifugation and redispersed in water. We stress that the variation in refractive index in the graded microbeads could cause additional light scattering; therefore, the dimensions of multilayer particles were determined only by quantitative image analysis of the SEM images using UTHSCSA Image Tool Version 1.28.

Results and Discussion

Core-Shell Particles with Polystyrene Cores.

Figure 1a shows a typical SEM image of monodisperse

microbeads synthesized by the homopolymerization of styrene (sample 1b, Table 1). Interfacial polymerization of HFBMA on the surface of polystyrene resulted in the production of particles with a nonspherical particle morphology. Figure 1b shows typical shapes of the resulting particles: the surface of the polystyrene microspheres was only partially engulfed with PHFBMA. Nonspherical shapes of particles obtained by emulsion polymerization have been previously observed for the latex beads comprising polymers with high interfacial tension between them.²⁴

All attempts to improve the morphology of the core-shell particles by varying the amounts of initiator and a cross-linking agent in the reaction mixture, and the temperature of polymerization did not lead to a significant improvement in particle shape and/or a uniform coverage of the PS core with PHFBMA or PHFBMA core with PS shell. To increase the extremely low solubility of HFBMA in water, we used cyclodextrin as an inverse phase transfer catalyst. No notable change was observed in particle shape and morphology.

Preparation of Core-Shell Particles by Copolymerization. To enhance compatibility of the alternating polymer layers, we have undertaken a copolymerization approach. The polymer layers with high refractive index were synthesized by the copolymerizing 90 wt % of styrene and 10 wt % of HFBMA. The layers with low refractive index were obtained by copolymerizing 10 wt % styrene and 90 wt % of HFBMA. The use of less than 10 wt % of the counterpart monomer led to the formation of microbeads with nonspherical shapes, as in Figure 1b. A greater than 10 wt % increase of the counterpart monomer could extend the decrease in refractive index contrast between the polymer layers.

Figure 2a shows a typical SEM image of the monodisperse polystyrene-rich particles with a number-average diameter of 190 nm (sample 1a). These particles were used as the seeds in the second stage. Core-shell microbeads with PHFBMA-rich shells (sample 2a) prepared from PS-rich seeds had a size of 380 nm and a spherical shape (Figure 2b), by contrast with particles synthesized from PS and PHFBMA homopolymers, as in Figure 1b. We continued the seeded emulsion polymerization for three consecutive stages producing samples 3a, 4a, and 5a (Figure 2c-e). A multistage polymerization was expected to lead to multilayer particles with a PS-rich core and four shells with alternating compositions (and thus periodically alternating refractive indices). After stage 5, the resulting particles had a spherical shape. Increase in particle size after each polymerization stage was from 190 to 360 nm and thus the estimated thickness of layers in the range from 95 to 180 nm (Table 2). The solid content of latex dispersions was somewhat lower than expected from the amount of monomers fed in the reaction flask and the solid content of seeds.

Figure 3a-c summarizes the results of characterization of the composition and properties of the composite particles vs the number of stages of their synthesis. Each graph in Figure 3 shows experimentally determined and anticipated particle property (based on the feeding ratios of styrene and HFBMA). Given that stage "0" produces latex cores, the number of stages (n) coincided with the number of layers in the microbeads.

Figure 3a shows the results of XPS analysis of surface composition of microbeads obtained in consecutive stages. For the particles synthesized in stages 0-4, a

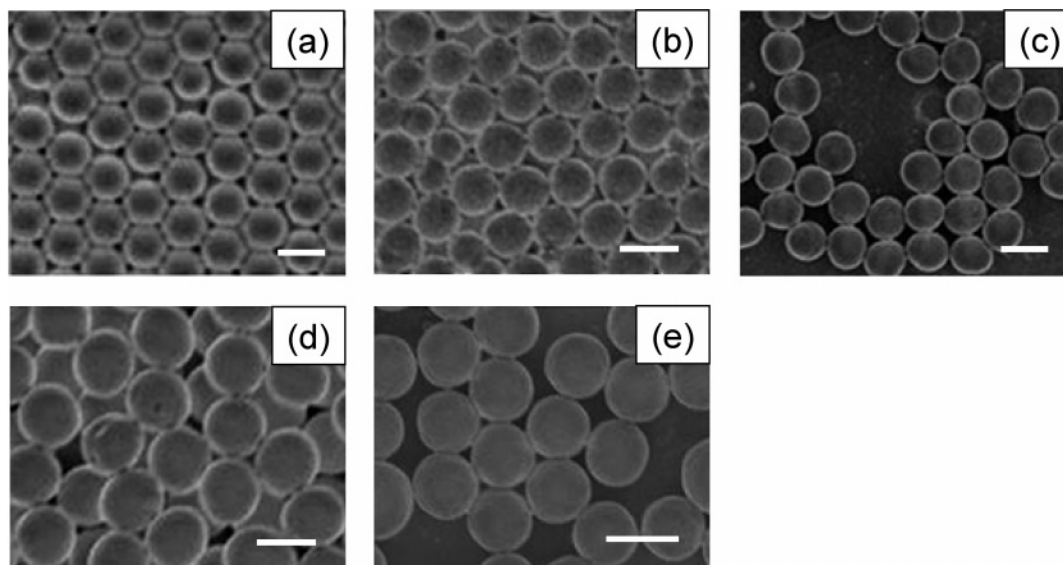


Figure 2. Typical SEM images of microspheres synthesized in different polymerization stages: (a) PS-rich cores (sample 1a), scale bar is 200 nm; (b) particle from (a) engulfed with PHFBMA-rich layer (sample 2a), scale bar is 400 nm; (c) particles from (b) engulfed with PS-rich layer (sample 3a), scale bar is 1.0 μm ; (d) particle from (c) engulfed with PHFBMA-rich layer (sample 4a), scale bar is 1.0 μm ; (e) particle from (d) engulfed with PS-rich fourth layer (sample 5a), scale bar is 1.5 μm .

Table 2. Particle Dimensions and Solid Content of Latex Suspensions

sample	solid content theoretical ^a (wt %)	solid content determined (wt %)	<i>n</i> -average diameter (SEM) (nm)	<i>n</i> -average thickness of outmost layer ^b (SEM) (nm)
1a	0.89	0.82 \pm 0.02	190 \pm 10	
2a	3.26	2.49 \pm 0.02	380 \pm 50	95
3a	2.95	1.86 \pm 0.21	700 \pm 40	160
4a	2.64	1.45 \pm 0.01	1060 \pm 100	180
5a	1.25	0.91 \pm 0.01	1400 \pm 120	170

^a Calculated from experimentally determined solid content of seeds and composition of reaction mixture assuming 100% conversion.

^b Calculated from the difference in *n*-average diameter of actual stage and prior stage.

periodic variation in the molar concentration of PHFBMA was observed, as expected for PHFBMA-rich and PS-rich layers. The composition of the alternating layers was consistent with the rationalized design of the graded microbeads. The content of PHFBMA in the outer shell, however, showed 2 to 19% deviation from the content expected from the molar feeding ratios of monomers.

In Figure 3b, the bulk composition of the composite PHFBMA–PS particles showed a periodic change correlating with the number of polymerization stages: the concentration of PHFBMA decreased when a monomer mixture enriched with styrene was used (stages 1–3) and increased when a monomer mixture was enriched with HFBMA (stages 2–4). The content of PHFBMA in the composite particles determined by ¹H NMR was 2–11% lower than in the monomer mixture.

In Figure 3c, the variation in thermal properties of the composite PHFBMA–PS microbeads confirmed the formation of particles with a multiphase structure. The glass transition temperatures of the PS-rich and PHFBMA-rich phases were 101.5 \pm 1.5 and 62.0 \pm 1.0 $^{\circ}\text{C}$, respectively. These values did not significantly change when the number of PS-rich and PHFBMA-rich layers was increased. The change of isobaric heat capacity ΔC_p at each transition was consistent with the relative bulk composition of particles. Typically, PHFBMA-rich particles showed a high value of ΔC_p at 60 $^{\circ}\text{C}$, while the change of heat capacity at 100 $^{\circ}\text{C}$ was smaller compared to PS-rich particles. The expected values of T_g of the PS-rich and PHFBMA copolymers were calculated using the Fox equation, based on the concentration of styrene

and HFBMA in the monomer mixture. We assumed a random PS–PHFBMA copolymer structure and the values of T_g of PHFBMA and PS of 65¹⁵ and 100.5 $^{\circ}\text{C}$,¹⁶ respectively. The calculated values showed at most a 10% deviation from the experimentally measured values of T_g 's of the composite particles.

To estimate the extent of compromise made to the refractive index contrast in the copolymerization approach, we first estimated the effective refractive indices of the copolymers with various compositions as¹⁷

$$n = \sqrt{\phi_{\text{PS}} n_{\text{PS}}^2 + \phi_{\text{polyHFBMA}} n_{\text{polyHFBMA}}^2} \quad (1)$$

where ϕ_{PS} and ϕ_{PHFBMA} are the volume fractions and n_{PS} and n_{PHFBMA} are the experimentally determined refractive indices at $\lambda = 589 \text{ nm}$ for PS and PHFBMA, respectively ($n_{\text{PS}} = 1.61$ and $n_{\text{PHFBMA}} = 1.386$, respectively). The homopolymers were obtained as described below. We note that the experimental values of refractive indices of PS and PHFBMA were close to the values of 1.59 and 1.38 reported in the literature^{16,17} for the corresponding polymers.

In Figure 4b, the solid lines show the variation in the refractive indices of copolymers enriched with PS (top line) or PHFBMA (bottom line) as a function of volume fraction of the counterpart polymer. For each composition of the copolymer, the difference in the refractive index represented the expected refractive index contrast between the adjacent layers. Copolymerization of the host monomer with a counterpart monomer led to a gradual decrease in refractive index contrast, which

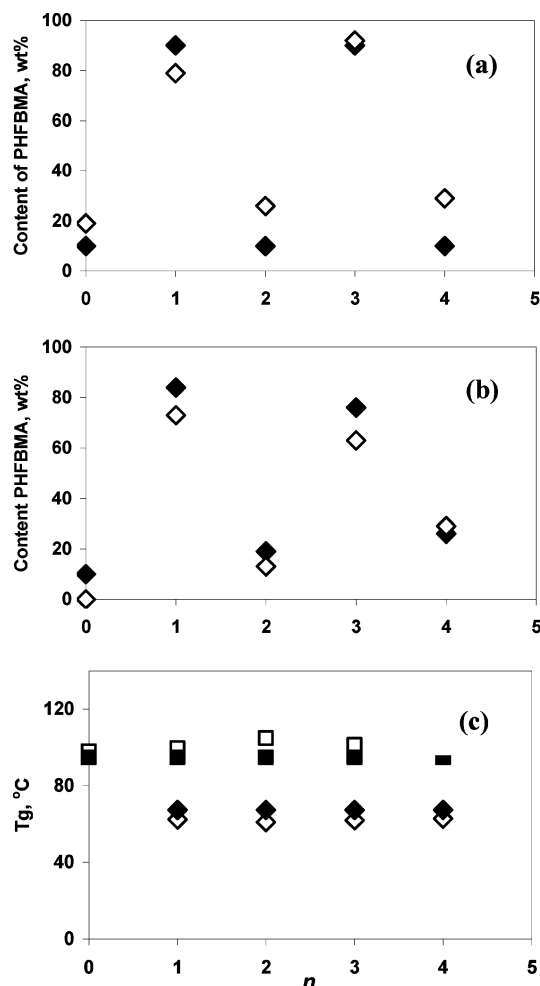


Figure 3. Variation in (a) surface composition, (b) bulk composition, and (c) glass transition temperatures of the multilayer particles following their multistage synthesis. Filled and empty symbols correspond to expected and experimentally determined copolymer composition, respectively. Stage "0" corresponds to the synthesis of particle cores.

approached zero for 50:50 volume ratio of the monomers. Clearly, the highest anticipated refractive index contrast was 0.22 for the combination of homopolymers PS and PHFBMA.

We experimentally determined the refractive indices of the alternating layers by synthesizing non-cross-linked particles comprising 0, 6.7, 85.3, and 100 vol % of PHFBMA (we used the density values of $\rho = 1.05 \text{ g cm}^{-3}$ and $\rho = 1.63 \text{ g cm}^{-3}$ for PS and PHFBMA, respectively).

We first examined the variation in refractive indices as a function of wavelength, λ , for the films obtained from these polymer particles: optical dispersion of polymers determined the optimized range of their performance in the resonator particles. In Figure 4b, PS showed greater optical dispersion than PHFBMA. The greater dispersion of PS than PHFBMA is due to effect of the low-energy $\pi \rightarrow \pi^*$ transitions of the phenyl group on the refractive index. In the entire spectral range studied, the difference between the refractive indices of PS-enriched and PHFBMA-enriched copolymers remained at 0.25 ± 0.05 . The experimental values of the refractive indices measured for the copolymers at $\lambda = 589 \text{ nm}$ were compared with the values calculated using eq 1. Good agreement was obtained between the calculated and measured refractive index values for both

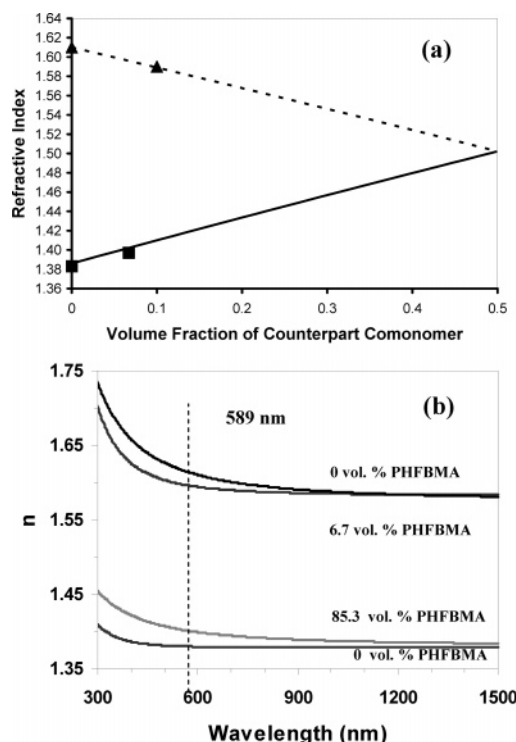


Figure 4. (a) Calculated and experimentally determined variation in refractive indices of counterpart polymers following their copolymerization in different volume ratios. PS-rich polymer: the refractive indices are represented by (—) for calculated and (▲) measured values. PHFBMA-enriched polymer: the refractive indices are represented by (—) for calculated and (■) measured values. The values of refractive indices were determined at $\lambda = 589 \text{ nm}$ and 20°C . (b) Variation of experimentally determined refractive indices of polymers as a function of wavelength. The dotted vertical line shows the wavelength at which the refractive indices are quoted in (a). The concentration of PHFBMA in the copolymer is 6.7 and 85.3 vol %.

PS-rich and PHFBMA-rich copolymers. Figure 4a also shows that the compromise in refractive index contrast in the multilayer microspheres due to the use of copolymerization approach was not substantial: in comparison to the refractive index difference for the homopolymers PS and PHFBMA of 0.23, the refractive index contrast achieved for the combination of PS-rich and PHFBMA-rich copolymers was 0.20. Finally, using good correlation between the experimental values of refractive indices and those calculated using eq 1, we estimated that the fluctuations in composition of high refractive index layers and low refractive index layers (found for the largest variation in the surface composition of the layers in Figure 3a) resulted in $\pm 8.5\%$ variation in refractive index contrast.

In summary, we report for the first time the synthesis of polymer multilayer particles with a strong periodic modulation of refractive indices of the alternating layers. We employed PS (a high refractive index component) and PHFBMA (a low refractive index component) to obtain four-layer $1400 \pm 120 \text{ nm}$ size particles. To enhance the compatibilization of these polymers, we used a copolymerization and a mixed initiator approaches and the addition of cyclodextrin to the dispersion medium. The resulting refractive index difference between the layers was slightly compromised due to copolymerization of high and low refractive index monomers. Future work will include the combination of counterpart polymers with a larger difference in refrac-

tive indices, better control over particle polydispersity, and synthesis of particles with a constant thickness of high and low refractive index layers.

Acknowledgment. We thank NSERC Canada for supporting the project under AGENO Program. C.P. thanks NSERC Canada for PGSD scholarship. We are grateful to Dr. W. Lau for his useful suggestions in polymer synthesis, H. Zhang for his assistance in DSC measurements, and Dr. J. Saarinen and Prof. J. Sipe for fruitful discussions.

References and Notes

- (1) (a) Brzozowski, L.; Sargent, E. H. *J. Opt. Soc. B: Opt. Phys.* **2000**, *17*, 1360–1365. (b) Siwick, B.; Kalinina, O.; Kumacheva, E.; Miller, D. R. *J. Appl. Phys.* **2001**, *90*, 5328–5338.
- (2) (a) Pham, H.; Gourevich, I.; Oh, J. K.; Jonkman, J. E. N.; Kumacheva, E. *Adv. Mater.* **2004**, *16*, 516–520. (b) Gourevich, I.; Pham, H.; Jonkman, J.; Kumacheva, E. *Chem. Mater.* **2004**, *16*, 1472–1479.
- (3) (a) Holtz, J. H.; Asher, S. A. *Nature (London)* **1997**, *389*, 829–832. (b) Lee, Y. J.; Pruzinsky, S. A.; Braun, P. V. *Langmuir* **2004**, *20*, 3096–3106.
- (4) (a) Yablonovich, E. *Phys. Rev. Lett.* **1987**, *58*, 2059–2062. (b) John, S. *Phys. Rev. Lett.* **1987**, *58*, 2486–2489.
- (5) (a) Yin, Y.; Lu, Y.; Gates, B.; Xia, Y. *J. Am. Chem. Soc.* **2001**, *123*, 8718–8729. (b) Kumacheva, E.; Golding, R.; Allard, M.; Sargent, E. H. *Adv. Mater.* **2002**, *14*, 221–224. (c) Golding, R. K.; Lewis, P. C.; Kumacheva, E.; Allard, M.; Sargent, E. H. *Langmuir* **2004**, *20*, 1414–1419.
- (6) Brady, D.; Papen, G.; Sipe, J. E. *J. Opt. Soc. Am. B* **1993**, *10*, 644–657.
- (7) Xu, Y.; Liang, W.; Yariv, A.; Fleming, G.; Lin, S. Y. *Opt. Lett.* **2004**, *29*, 424–426.
- (8) See, e.g.: (a) Leung, P. T.; Pang, P. K. *J. Opt. Soc. Am. B* **1996**, *13*, 805–817. (b) Lee, K. M.; Leung, P. T.; Pang, K. M. *J. Opt. Soc. Am. B* **1999**, *16*, 1418–1430. (c) Burlak, G. N. *Phys. Lett. A* **2002**, *299*, 94–101.
- (9) Farrer, R. A.; Copeland, G. T.; Previte, M. J. R.; Okamoto, M. M.; Miller, S. J.; Fourkas, J. T. *J. Am. Chem. Soc.* **2002**, *124*, 1994–2003.
- (10) Caruso, F.; Lichtenfeld, H.; Donath, E.; Mohwald, H. *Macromolecules* **1999**, *32*, 2317–2328.
- (11) Dimonie, V. L.; Daniels, E. S.; Shaffer, O. L.; El-Aasser, M. S. In *Emulsion Polymerization and Emulsion Polymers*; Lowell, P. A., El-Aasser, M. S., Eds.; Wiley: Chichester, 1997; Chapter 9, pp 293–3126.
- (12) Kirsch, S.; Landfester, K.; Shaffer, O.; El-Aasser, M. S. *Acta Polym.* **1999**, *50*, 347–362.
- (13) Wang, Z. Y.; Paine, A. J.; Rudin, A. *J. Polym. Sci., Part A: Polym. Chem.* **1995**, *33*, 1597–1606.
- (14) (a) Nelliappan, V.; El-Aasser, M. S.; Klein, A.; Daniels, E. S.; Roberts, J. E. *J. Polym. Sci., Part A: Polym. Chem.* **1996**, *34*, 3173–3181. (b) Rajatapitu, P.; Dimonie, V. L.; El-Aasser, M. S.; Vratsanos, M. S. *J. Appl. Polym. Sci.* **1997**, *63*, 205–219.
- (15) (a) Durant, Y. G.; Sundberg, E. J.; Sundberg, D. C. *Macromolecules* **1997**, *30*, 1028–1032. (b) Ivarsson, L. E.; Karlsson, O. J.; Sundberg, D. C. *Macromol. Symp.* **2000**, *151*, 407–412. (c) Stubbs, J.; Karlsson, O.; Jonsson, E. J.; Sundberg, E.; Durant, Y.; Sundberg, D. *Colloids Surf. A* **1999**, *153*, 255–270.
- (16) Gaynor, J.; Schuenemann, G.; Schuman, P.; Harmon, J. P. *J. Appl. Polym. Sci.* **1993**, *50*, 1645–1653.
- (17) Seferis, J. C. *Polymer Handbook*, 3rd ed.; Brandrup, J., Ed.; Wiley: New York, 1989; Vol. VI, pp 451–461.
- (18) Stosberg, J.; Ritter, H. *Macromol. Chem. Phys.* **2002**, *203*, 812–818.
- (19) Kalinina, O.; Kumacheva, E. *Macromolecules* **2001**, *34*, 6380–6386.
- (20) O'Callaghan, K. J.; Paine, A. J.; Rudin, A. *J. Appl. Polym. Sci.* **1995**, *58*, 2047–2055.
- (21) (a) Egen, M.; Braun, L.; Zentel, R.; Tannert, K.; Frese, P.; Reis, O.; Wulf, M. *Macromol. Mater. Eng.* **2004**, *289*, 158–163. (b) Comoretto, D.; Marabelli, F.; Soci, C.; Galli, M.; Pavarini, E.; Patrini, M.; Andreani, L. C. *Synth. Met.* **2003**, *139*, 633–636.
- (22) Pateta, O.; Bohm, S.; Cirkva, V. *J. Fluorine Chem.* **2000**, *102*, 159–168.
- (23) Dahman, Y.; Puskas, J. E.; Margaritis, A.; Merali, Z.; Cunningham, M. *Macromolecules* **2003**, *36*, 2198–2205.
- (24) (a) Giani, E.; Sparnacci, K.; Laus, M.; Palamone, G.; Kape-liouchko, V.; Arcella, V. *Macromolecules* **2003**, *36*, 4360–4367. (b) Cairns, D. B.; Khan, M. A.; Perruchot, C.; Riede, A.; Armes, S. P. *Chem. Mater.* **2003**, *15*, 233–239.

MA047446A